

## Injection and Thermalization of Hot Electrons in Solid, Liquid, and Gaseous Helium at Low Temperatures\*

David G. Onn<sup>†</sup> and M. Silver

*Department of Physics, University of North Carolina, Chapel Hill, North Carolina 27514*

(Received 9 November 1970)

Thin-film cold-cathode emitters were used to inject electrons into solid helium, liquid helium under pressure, and gaseous helium at 4.2 and 20 °K. The cross section for the interaction of the injected quasifree electrons with the helium was deduced by use of an appropriate model for the thermalization of the electrons, and sundry other parameters of the quasifree state, such as its lifetime and collision frequency of the electron therein, were deduced. The cross section derived is within a factor of 2 of the value for the elastic scattering cross section for the isolated atom. The description of the scattering and thermalization process is dependent only on the helium atomic density and is independent of phase.

### I. INTRODUCTION

In an earlier paper<sup>1</sup> we examined the thermalization of hot electrons emitted from a cold-cathode emitter into liquid helium under saturated vapor pressure. We have extended this work to liquid helium under pressures up to 100 atm, to solid helium, and to gaseous helium at liquid-hydrogen temperature and high pressure. In the last case, the numerical atomic density achieved was comparable to that in the liquid helium. A considerable advance is possible beyond our previous work because of our increased knowledge of the energy distribution of the electrons emitted from our cathodes, because of the much wider range of helium densities studied, and by comparison of the thermalization process in the three helium phases.

There is considerable evidence, theoretical and experimental,<sup>2-9</sup> that the negative ion in liquid helium consists of a self-trapped electron in a "bubble" of about 15–20-Å radius, with a well depth of approximately 1 eV at 4.2 °K. This structure is energetically preferred to its alternative, a quasifree nonlocalized electron, because of the strong short-range repulsive interaction between the electron and the helium atoms. Recent calculations have shown that the bubble state will be preferred in solid helium also.<sup>10</sup>

Shalnikov first succeeded in obtaining currents in solid helium by the use of a radioactive source.<sup>11</sup> He later studied the temperature dependence of the current.<sup>12</sup> From these measurements the estimated mobility of the electron in solid helium has the same order of magnitude as the mobility in liquid helium, providing some experimental evidence that the thermalized state may also be a bubble.

### II. THEORY

The model that we use for describing the injection process has been described previously,<sup>1</sup> and

the current-voltage characteristics deduced. Both will be reviewed here for completeness and in order to point out developments in interpretation in the present work.

Figure 1 is a schematic of the injection model. The injected electrons are initially quasifree and will lose their energy in some manner to the helium until thermalized. The thermalized state is not necessarily the final bubble state, but at least represents a large drop in the mobility of the electron, of the type that Sanders and Levins<sup>4</sup> have observed and interpreted as due to a fully formed bubble or an incipient bubble as proposed by Silver, Hernandez, and Onn<sup>13</sup> and expanded upon by Hernandez and Silver.<sup>14</sup> The thermalization may be characterized by a "range"  $x_0$ , which is comparable to  $x_M$ , the distance from the injecting surface to the peak in the potential caused by the applied and image potentials,

$$x_M = (e/4E_A)^{1/2}, \quad (1)$$

where  $E_A$  is the applied field.

It is confirmed from this study that all of the energy of the injected electron cannot be dissipated by elastic scattering within the range  $x_0$ , which indicates that a final inelastic process occurs at range  $x_0$ . If the effective momentum exchange mean free path for scattering of the quasifree electrons is symbolized by  $x_x$ , then the current collected would be

$$I_c = I_\infty e^{-x_M/x_0} = \frac{I_{\text{vac}} A}{1 + (6/\pi)^{1/2} x_0/x_x} e^{-x_M/x_0}, \quad (2)$$

where  $A$  (for attenuation) represents the effect of the electron helium barrier. The barrier will attenuate the vacuum current ( $I_{\text{vac}}$ ) because, of all the emitted electrons, only the more energetic electrons can penetrate into the helium. The en-

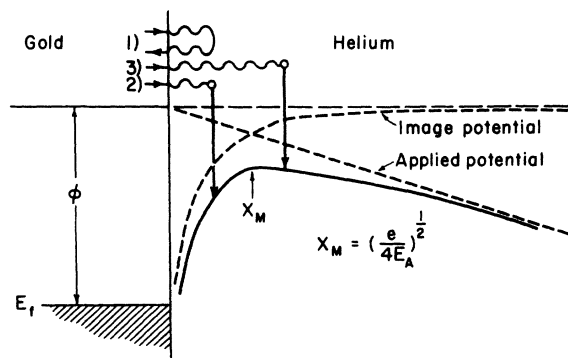


FIG. 1. Schematic of the injection model. For clarity, the electron-helium barrier is suppressed, and may be taken as the total effective work function.

term in parentheses in the denominator of the preexponential is the effect of back diffusion of the injected hot electrons.<sup>15,16</sup> Note that in equation (2) a typographical error from Eqs. (20) and (21) of Ref. 1 has been corrected.  $I_\infty$  is the extrapolated current for infinite applied field.

In Ref. 1  $x_x$  and  $A$  were both unknown. Because of these uncertainties, we assumed that

$$x_x = x_s = 1/n\sigma_s,$$

where  $x_s$  and  $\sigma_s$  are the mean free path (mfp) and cross section for elastic scattering, and  $n$  is the atomic density. Now that we have an estimate of  $A$  under the assumption that the electron-helium barrier calculations are correct, it is possible to obtain information on  $x_x$  and compare it with  $x_s$  and other estimates of the relevant mfp. This would also enable us to evaluate whether a simple perturbation approach to scattering including atom-atom correlation used so successfully in argon<sup>17,18</sup> is also applicable to helium.

It is also possible to determine the lifetime before thermalization ( $\tau$ ) of the quasifree electrons, and the collision frequency ( $\nu$ ) which have implications in other discussion of the interactions of charges with liquid helium.<sup>13,14</sup> The number of collisions undergone by the electron before thermalization is

$$N_c = 6x_0^2/x_x^2, \quad (3)$$

$$\tau = 6x_0^2/cx_x, \quad (4)$$

$$\nu = N_c/\tau = c/x_x, \quad (5)$$

where  $c$  is the average velocity of the injected electrons. Note that Eq. (3) is a correction of Eq. (19b) of Ref. 1. Our results will be presented in the form of values for  $x_0$ ,  $x_x$ ,  $\sigma_x$ ,  $\nu$ , and  $\tau$  as functions of the helium atomic density in the three phases of helium studied.

It should be noted that in Eq. (2) we have re-

tained the numerical factor  $(6/\pi)^{1/2}$  rather than using 1.5, which is used by Loeb<sup>16</sup> and by Theobald<sup>19</sup>; however, the numerical difference is small.

### III. EXPERIMENTAL

The experimental arrangements and circuits used were essentially the same as those used in the earlier paper.<sup>1</sup> A new sample chamber of thick stainless steel was used for the high-pressure runs. A copper cold-finger insert provided a "cold spot" for mounting the emitters. The emitter-to-collector distance was reduced to 0.25 mm so that higher fields could be obtained within the operating limits of our electrometers.

The emitters used were of the same construction also (Al-Al<sub>2</sub>O<sub>3</sub>-Au), but the oxide thickness was standardized and most of the emitters operated at the same applied voltage (10.2 V) which resulted in a repeatable current in vacuum ( $I_{vac}$ ) of about 3000 pA. No emitters were used with thickness requiring driving voltages of less than 8 V, since it is known that  $x_0$  decreases quite rapidly for such thin emitters.<sup>1</sup> This is probably due to the narrow energy distributions from the thinner emitters, which allows a considerable number of the emitted electrons of lower energy to thermalize without any inelastic process before reaching  $x_M$ , thus effectively lowering  $x_0$ . This fraction could be calculated and corrected for, but can be neglected with emitters operating above about 8 V.

The cryostat was cooled in a Dewar containing liquid helium or hydrogen, and the Dewar could be pressurized to obtain data above 4.2°K with liquid helium, though this method was limited by

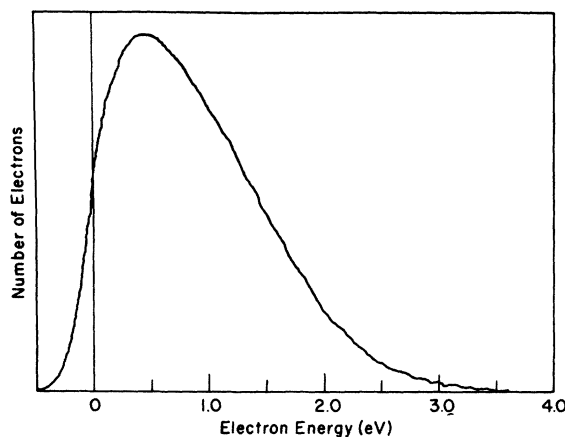


FIG. 2. Energy distribution of emitted electrons from an emitter operated at 9.4 V. This distribution was obtained using a retarding voltage technique with planar geometry. Energy scale on the abscissa corresponds to the retarding voltage. Zero was taken at the zero applied retarding voltage.

TABLE I. Attenuation factor  $A$  [Eq. (2)] and average injection velocity  $C$  calculated by Burdick's method (Ref. 7).

Electron-helium barrier $E_B$ (eV)	Reciprocal helium atomic density $N^{-1}$ ( $10^{-22}$ cm <sup>3</sup> atom <sup>-1</sup> )	Attenuation factor $A$	Average injection velocity $C$ ( $10^7$ cm sec <sup>-1</sup> )
0.6	0.760	0.63	4.85
0.8	0.595	0.51	4.63
1.0	0.490	0.40	4.45
1.2	0.420	0.31	4.24
1.4	0.373	0.23	4.10
1.6	0.335	0.16	3.90
1.8	0.305	0.11	3.70

thermal instabilities. The sample container was pressurized from a helium cylinder, and the pressure read from a precision dial pressure gauge. No special measures were taken to purify the helium used, but confirmation tests with ultrapure helium indicate that impurities do not affect our results.

The energy distributions of the emitters were obtained by use of a modulated grid-retarding potential method. Further details of the method and of the distributions will be given elsewhere.<sup>20</sup> A typical energy distribution for the type of emitter and operating conditions of our experiment is shown in Fig. 2. From such a distribution it is possible to calculate approximately the fraction of the total current able to be injected over a known barrier, and also to calculate the average velocity of the electrons injected. Typical results are listed in Table I. The precise shape of the energy distribution at low energies is difficult both to determine and, at present, to interpret, and may contain instrumental effects from the analyzer design.<sup>20</sup> However, this region contributes relatively little to the total current and, since we are working with potential barriers of the order of 1 eV, causes only slight uncertainty in both the fraction injected and the average energy.

A possible other source of error is in the "aging" effects experienced in working with our emitters.<sup>20</sup> Although these effects, which affect both  $I_{vac}$  and the details of the energy distribution, can be ameliorated to some extent by long periods of operation of the emitter in vacuum before use for data collection, we have found no way of determining the effects of pressure on the emitters themselves. We observed generally that the emitters did age more rapidly under high pressures, particularly at 20°K, and showed a marked reduction (10–15%) in emission after operation at high pressure for some time. Corrections for this were made by reducing the pressure periodically to some stan-

dard pressure to provide a reference point to determine  $I_{vac}$ .

Solid helium was made in two ways. The sample was pressurized slowly while the liquid was below the  $\lambda$  point until the solidification curve was crossed. This method has the disadvantage that once the solid is formed, the pressure applied is no longer transmitted easily to the small volume of the experimental chamber used for the injection experiments. Currents obtained with increasing pressure on the solid corresponded to helium densities at which the solid first formed. However, above a critical pressure in the region of 45 atm the current decreased rapidly, became unstable, or disappeared, but, after annealing for some time close to the melting curve, the current stabilized to a new value, though the sample density was not known. Similar effects were reported by Shalnikov.<sup>11</sup>

The solid was also formed by cooling the liquid under pressure. This could not be done at constant volume with the present apparatus, so that there was still some uncertainty in the density. In both methods, the use of a cold-finger copper support for the emitter, which was in good thermal contact with the bath, combined with the thick-walled stainless-steel sample chamber ensured that the solid was first formed on the emitter and finger. Our main concern in studying injection is with the helium in contact with the emitter surface.

#### IV. RESULTS

##### A. Liquid under Pressure

We obtained characteristics of collected current  $I_c$  as a function of the electric field  $E_A$  applied to the helium sample between the emitter and the collector; a typical set of data is shown in Fig. 3. The abscissa in both plots has been reduced to show the peak potential distance  $x_M$  obtained from Eq. (1). From these plots we can determine the thermalization distance  $x_0$  directly from the inverse of the slope, and, from the intercept on the current axis, we can determine the current  $I_\infty$  available at (unattainable) infinite applied field. It is clear from Fig. 3 that both  $x_0$  and  $I_\infty$  decrease rapidly as the density of the helium is increased.

The extrapolation of the data lines back to the current axis intercept becomes increasingly difficult as  $x_0$  decreases (the slope increases) because of the experimental limits imposed by the maximum applied field and the noise level at low currents. These two limits combine to reduce the range of  $x_M$  over which  $I_c$  can be measured accurately. The variation of  $I_\infty$  as a function of density is now well outside the errors due to the extrapolation difficulties. This was not true in earlier work<sup>1</sup> and spurious variations of  $I_\infty$ , due

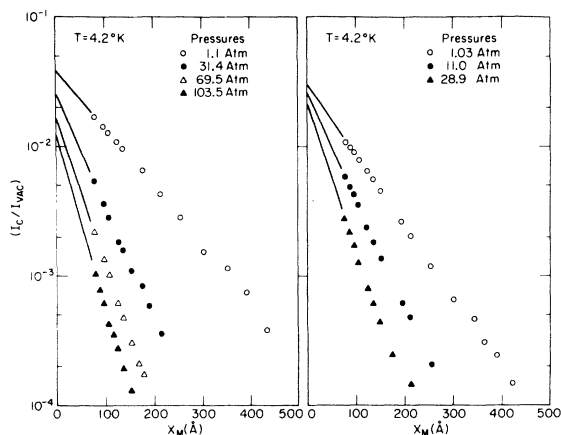


FIG. 3. Collected current data for liquid helium under pressure at 4.2°K. The two sets of data are for different emitters. Typical slight variations in  $x_0$  and  $I_c/I_\infty$  are illustrated by these two sets of data.

in part to unrecognized aging effects in our emitters, were given too much weight in interpretation.

There still remains some variation in  $I_\infty$  from one emitter to another which is probably due to some variations in the energy distribution. But, for each emitter, the variation of  $I_\infty$  with helium density is repeatable relative to  $I_\infty$  at the standard conditions of liquid at 4.2°K and one atmosphere pressure. Accordingly we selected this value of  $I_\infty$  as a standard reference  $I_1$ , finally averaging the results of many emitters for which  $I_1$  varied from  $0.07I_{vac}$  to  $0.03I_{vac}$ . The results will be summarized below.

#### B. Solid Helium

Collected current characteristics  $I_c$  vs  $x_M$  for helium compressed at 1.5°K are shown in Fig. 4. A clear decrease in current occurs at the pressure at which the solid forms. The current increased sharply again as the pressure was released. A similar effect was observed by Shalnikov.<sup>11</sup> The discontinuities we observe are, however, always reproducible for a given field strength, and furthermore the same current increase is observed at 1.5°K when a solid sample melts after formation by increasing pressure at temperatures just below the  $\lambda$  point. This strongly suggests that we are observing the true current change due to solidification of the helium.

A characteristic for the current in the solid helium is shown in Fig. 4 and has a determinable value of  $x_0$  and  $I_\infty$ , though the experimental limitations described above for the dense liquid apply once more. The variations of  $x_0$  and  $I_\infty$  in the liquid at this temperature are similar to those at 4.2°K. No detectable discontinuity in  $x_0$  or  $I_\infty$  was seen at the  $\lambda$  line. As will appear later, the discontinuity

in current at solidification is due to the density change, which causes a change in the barrier to injection as well as in the scattering mfp.

In order to obtain  $x_0$  and  $I_\infty$  for various solid densities, samples were prepared by cooling the pressurized liquid. As a result the densities of the solid are not as well known as for the liquid, but the relative accuracy of determination of  $x_0$  and  $I_\infty$  make this unimportant at present. The values of these two parameters agreed with those expected for a liquid at the same densities.

#### C. High-Density Gas

Characteristics obtained in pressurized helium gas at liquid-hydrogen temperatures are shown in Fig. 5. At pressures above about 40 atm the characteristics are similar to those obtained in the liquid at the same atomic densities, in that we can determine  $x_0$  from the slope, and  $I_\infty$  depends on density as it does in the liquid. At pressures below about 40 atm the characteristics take on a form typical of characteristics obtained in many other gases at higher temperatures, and in helium gas at 77°K. This more complex behavior will be discussed in a separate publication.<sup>21</sup> It should be noted, however, that the apparent change in the form of the characteristic at 40 atm (about  $1.4 \times 10^{22}$  atoms  $\text{cm}^{-3}$ ) is not necessarily comparable to the large mobility drop observed by Sanders and Levine<sup>4</sup> at approximately an order of magnitude lower density.

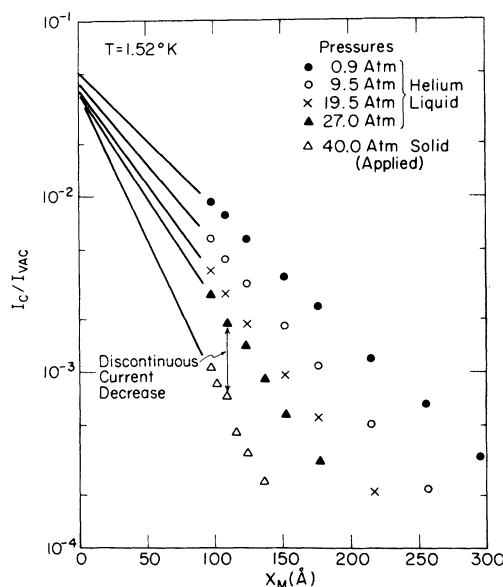


FIG. 4. Collected current data for liquid helium at 1.52°K under pressure, and for solid helium. Although the applied pressure for these data was 40 atm the helium density was that at solid formation at approximately 28 atm (see text).

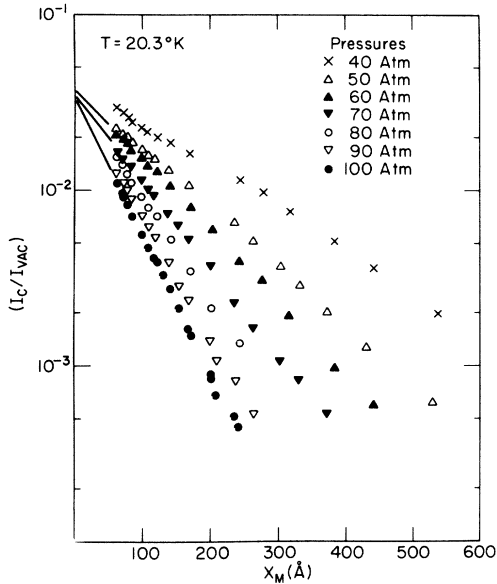


FIG. 5. Collected current characteristics for helium gas under pressure at 20.3 °K.

We have extensively studied the current-voltage characteristics obtained by electron injection into helium vapor, saturated and unsaturated, at 4.2 °K in the region where Sanders and Levine observed the mobility drop. We observed only a steady decrease in collected current as a function of increasing atomic density. There is not necessarily any disagreement between our results and Sanders and Levine's at the lower density. Our results do

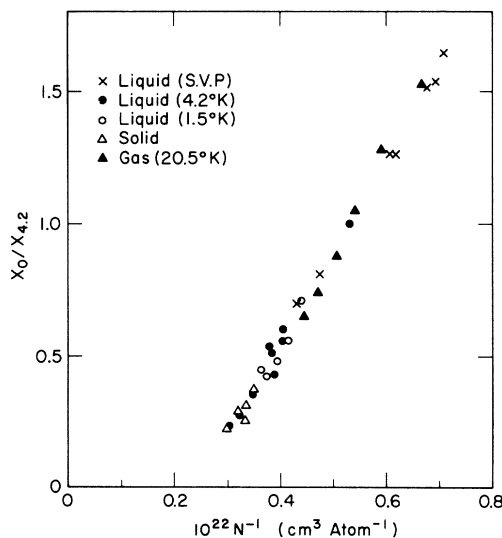


FIG. 6. Summary of values of the thermalization range for varying reciprocal atomic densities in three phases of helium.

not imply that there is no bubble, only that the time of formation may be relatively long so that  $x_0$  would be large compared with  $x_M$ . However, we have observed<sup>21</sup> a sharp decrease in collected current in high-density hydrogen gas at both 77 and 160 °K at an atomic density of about  $1.8 \times 10^{21}$  atoms  $\text{cm}^{-3}$  showing that this method is capable of determining changes in electron states at these densities if  $x_0$  is short enough. Work in this area is continuing, and the results will be collated later.<sup>21</sup>

## V. DISCUSSION

Figures 6 and 7 combine the results of many sets of collected current characteristics. In Fig. 6, values of  $x_0$  in the solid, liquid, and gaseous phases are plotted against the reciprocal atomic density ( $N^{-1}$ ) of the helium. All points are normalized to the value of  $x_0$  obtained in the liquid for each emitter at 4.2 °K and 1 atm pressure, except that in the case of the gas normalization was made to the  $x_0$  obtained at the same numerical density. The atomic densities for the gas phase were computed from the known virial coefficients.<sup>22</sup>

From Fig. 6, the thermalization range for the injected electron in dense helium  $x_0$  is seen to vary with density in the same way for all three phases, with no discontinuity for any phase boundary. The sole determinant of  $x_0$  appears to be the atomic density of the helium. The intercept on the reciprocal density axis has little direct physical meaning however, being to some extent dependent on the details of the energy distribution, though this is concealed by the normalization. The intercept corresponds to immediate thermalization, but the barrier to injection at these densities has increased so much that the remaining electrons have a very narrow energy distribution, leading to difficulties similar to those discussed earlier for thin oxide emitters. In addition, the diffusion

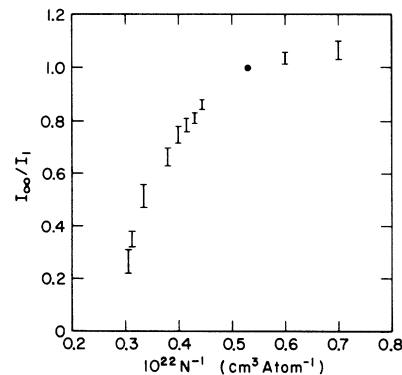


FIG. 7. Variation of the "infinite field intercept," relative to its value in liquid at 4.2 °K and 1 atm, as a function of reciprocal atomic density in the liquid.

model on which Eq. (2) is based contains assumptions no longer valid in this region.

Figure 7 shows the dependence of the normalized "infinite field" current ( $I_\infty/I_1$ ) as a function of  $N^{-1}$  for the liquid under pressure. Points obtained in the solid and dense gas follow the same curve. The error bars increase at high and low densities because of the difficulties of extrapolation, which can only partially be overcome by accumulation of data from many runs. The coincidence of  $I_\infty/I_1$  values for the three phases points out the numerical density as the sole determinant of the preexponential factor in Eq. (2). The combination of the evidence from Figs. 6 and 7 implies that the scattering and final thermalization of the quasifree injected electrons is quite independent of the phase, and depends only on the atomic density of the helium. This does not mean that the final thermalized state is identical in each phase, though calculations and experiment suggest that this may be the case.<sup>10,12</sup>

We have been apprised of some data obtained by Surko and Reif<sup>23,24</sup> on secondary-electron emission from a gold electrode due to bombardment by neutral excitations in liquid helium. Those observations were made in the temperature range 0.35–0.55 °K. The derived value of  $x_0$  from their current-versus-voltage characteristic is approximately 55 Å which is in very good agreement with our data at higher temperature but the same density. This lends support to the notion that density is the controlling factor in determining the thermalization range.

We can use the information from Figs. 6 and 7, together with a knowledge of the electron-helium barrier as a function of atomic density to obtain values of the scattering cross section for the quasifree electrons before they thermalize, and to determine the quasifree-state lifetime  $\tau$  and collision frequency  $\nu$ .

Several methods exist for calculating the effective electron-helium barrier.<sup>3,4,7</sup> We used the method of Burdick<sup>7</sup> to determine the dependence

of the barrier on atomic density, and made the assumption that once the barrier was known this determined the fraction of a typical electron energy distribution that was injected into the helium, thus determining the factor  $A$  in Eq. (2). We neglected any possible variation in  $A$  due to varying transmission coefficient due to, for instance, the Kapitza layer. The resulting values of  $A$  and the average injection velocity are summarized in Table I for a sample energy distribution.

From the above-determined values of  $A$ ,  $x_0$ , and  $I_\infty/I_{\text{vac}}$  we can calculate the scattering mfp,  $x_x$ , as a function of helium atomic density from Eq. (2). The cross section for scattering is determined from Eq. (3), and Eqs. (4) and (5) determine the lifetime and collision frequency. Finally, as a consistency check we can calculate the ratio  $\nu/N$ , which should be constant. The results of these calculations are summarized in Table II.

The values of the cross section lie within a factor of 2 of the value obtained in gas studies at higher temperatures,<sup>25</sup> which agree in turn extremely well with calculations.<sup>26</sup> These calculations in no way include atom-atom correlation as was done by Lekner<sup>17</sup> and by Cohen<sup>14</sup> for electron scattering in argon. A blind application of this perturbation approach yields too small a cross section by a factor of about 10 and one which depends upon temperature which is not found experimentally. The correct formulation of the problem of scattering of quasifree electrons in liquid helium where the electron-medium interaction is strong is yet to be made. In any case, the cross section is approximately constant over the density range studied with a possible higher cross section at the highest densities studied (see Table II).

The quasifree electron state lifetimes listed in Table II are more certain than in our previous paper<sup>1</sup> because of the added knowledge of the injected electron energy distribution. The lifetime clearly decreases rapidly with increasing helium density, whereas the collision frequency rises as

TABLE II. Results of calculations.

Reciprocal helium atomic density $N^{-1}$ ( $10^{-22}$ cm <sup>3</sup> atom <sup>-1</sup> )	Range $x_0$ (Å)	mfp $x_x$ (Å)	Calculated cross section $\sigma_x$ ( $10^{-16}$ cm <sup>2</sup> )	Quasifree- state lifetime $\tau$ (psec)	Collision frequency $\nu$ ( $10^{14}$ sec <sup>-1</sup> )	Consistency $\nu/N$ (arbitrary units)
0.760	155 ± 10	21 ± 4	3.6 ± 0.7	1.4 ± 0.3	2.3 ± 0.4	1.8
0.595	111 ± 8	18 ± 3	3.3 ± 0.5	0.9 ± 0.2	2.6 ± 0.4	1.5
0.490	77 ± 4	14 ± 3	3.5 ± 0.7	0.6 ± 0.15	3.2 ± 0.4	1.6
0.420	55 ± 4	11.5 ± 2	3.7 ± 0.6	0.4 ± 0.1	3.7 ± 0.4	1.6
0.373	40 ± 4	10 ± 2	3.7 ± 0.7	0.25 ± 0.1	5 ± 1	1.8
0.335	29 ± 5	7 ± 2	5 ± 1.5	0.15 ± 0.1	7 ± 2	2.2
0.305	20 ± 7	45 ± 2	7 ± 3	...	...	...

expected. The consistency check shows  $\nu/N$  to be constant within our experimental error, except in the case of the highest densities studied. Whether this increase is real or not is yet to be determined.

From Eq. (5) and the values of  $\tau$  and  $\nu$  it is possible to calculate the number of collisions of the quasifree electron within the range  $x_0$ . This varies from about 300 at the lowest densities, to less than 100 at the highest. If these collisions are elastic, (and the calculated cross sections show this to be essentially true) then the energy lost in such a low number of collisions cannot account for all of the energy of the injected electrons, showing that a final inelastic process must account for the thermalization.

#### VI. SUMMARY AND CONCLUSIONS

Thin-film cold-cathode emitters have been used as sources of electron current in solid helium, liquid helium, and high-pressure gaseous helium. The thermalization of the injected hot electrons from their quasifree state is independent of the phase of helium, at least as reflected by the parameters that we determine. The primary determinant of the lifetime of the quasifree state and the collision frequency of the electron in this state is the helium atomic density. This fact provides further

evidence that the thermalized electron state is also independent of the phase, as calculations and mobility values had indicated.

The quasifree-state lifetimes determined are in the order of picoseconds, or less, with the lifetime decreasing very rapidly with increasing helium density. The collision frequency is proportional to the atomic density, which is reasonable. By knowing the energy distribution of the injected electrons we have been able to calculate the scattering cross section for the quasifree electrons before thermalization. The value obtained lies within a factor of 2 of the elastic scattering cross section obtained by conventional techniques and calculations.

The technique of injecting hot electrons into insulating media from cold-cathode emitters has been improved by knowledge of the energy distribution of the emitted electrons, and may readily be extended to many other systems.

#### ACKNOWLEDGMENTS

The authors wish to express their appreciation to Professor H. Meyer of Duke University and Professor J. Hernandez and Professor K. S. Dy of the University of North Carolina at Chapel Hill for their helpful discussions.

\*Work supported by the Army Research Office, Durham, the National Science Foundation, and the Materials Research Center of the University of North Carolina under Contract No. SD-100 from the Advanced Research Projects Agency.

†Present address: Department of Physics, University of Delaware, Newark, Del. 19711.

<sup>1</sup>David G. Onn and M. Silver, Phys. Rev. **183**, 295 (1969).

<sup>2</sup>R. A. Ferrel, Phys. Rev. **108**, 167 (1957).

<sup>3</sup>K. Hiroike, N. R. Kestner, S. A. Rice, and J. Jortner, J. Chem. Phys. **43**, 2625 (1965).

<sup>4</sup>J. L. Levine and T. M. Sanders, Phys. Rev. **154**, 138 (1967).

<sup>5</sup>J. A. Northby and T. M. Sanders, Phys. Rev. Letters **18**, 1184 (1967).

<sup>6</sup>C. V. Briscoe, S.-I. Choi, and A. T. Stewart, Phys. Rev. Letters **20**, 493 (1968).

<sup>7</sup>B. Burdick, Phys. Rev. Letters **14**, 11 (1965).

<sup>8</sup>T. Miyakawa and D. L. Dexter, Phys. Rev. A **1**, 513 (1970).

<sup>9</sup>W. B. Fowler and D. L. Dexter, Phys. Rev. **176**, 337 (1968).

<sup>10</sup>M. H. Cohen and J. Jortner, Phys. Rev. **180**, 238 (1969).

<sup>11</sup>A. I. Shalnikov, Zh. Eksperim. i Teor. Fiz. **41**, 1059 (1961) [Sov. Phys. JETP **14**, 755 (1962)].

<sup>12</sup>E. Ifft, L. Mezhev-Deglin, and A. Shalnikov, in

*Proceedings of the Tenth International Conference on Low Temperature Physics* (Foreign Languages Publishing House, Moscow, 1967), Vol. 1, p. 224.

<sup>13</sup>M. Silver, J. P. Hernandez, and David G. Onn, Phys. Rev. A **1**, 1268 (1970).

<sup>14</sup>M. Silver and J. P. Hernandez, Phys. Rev. (to be published).

<sup>15</sup>J. J. Thomson, *Conduction of Electricity Through Gases* (Cambridge U. P., London, 1928), 3rd ed., Vol. 1, p. 466.

<sup>16</sup>L. Loeb, *Basic Processes of Gaseous Electronics* (California U. P., Berkeley, Calif., 1955), Chap. VII.

<sup>17</sup>J. Lekner, Phys. Rev. **158**, 130 (1967).

<sup>18</sup>M. H. Cohen and J. Lekner, Phys. Rev. **158**, 305 (1967).

<sup>19</sup>J. K. Theobald, J. Appl. Phys. **24**, 123 (1953).

<sup>20</sup>David G. Onn and P. Smejtek (unpublished).

<sup>21</sup>M. Silver, P. Smejtek, and David G. Onn (unpublished).

<sup>22</sup>G. A. Cook, *Argon, Helium and the Rare Gases* (Interscience, New York, 1961), p. 261.

<sup>23</sup>C. M. Surko and F. Reif, Phys. Rev. **175**, 229 (1968).

<sup>24</sup>We are grateful to Dr. C. M. Surko for making these data from his Ph.D. thesis available to us.

<sup>25</sup>D. E. Golden and H. W. Bandel, Phys. Rev. **138**, A14 (1965).

<sup>26</sup>T. F. O'Malley, Phys. Rev. **130**, 1020 (1965).